MODULATION TRANSFER AND SCINTILLATION LIMITATIONS IN GAMMA-RAY IMAGING

Eldon L. Keller and John W. Coltman

Westinghouse Research Laboratories, Pittsburgh, Pennsylvania

Imaging of gamma-emitting radioisotopes was seriously approached in the late 1940s. Copeland and Benjamin (*1*), for example, accomplished this in 1949 using pinhole collimation and x-ray film. Although Anger (*2*) achieved improved sensitivity in 1952 by using a sodium iodide converter and a blue-sensitive photographic plate, pinhole devices of this nature were not of practical value. The development of the rectilinear scanner by Cassen and co-workers (*3*) in 1951 provided the impetus for the widespread use of radioisotopes for curioscopic (*4*) examination. Since that time, instrumentation for gamma-ray imaging has been continually improved. The recent development of stationary cameras (*5*) has further enhanced the diagnostic capability of the nuclear-medicine clinician by letting him record multiple organ views from single radiopharmaceutical administrations and perform dynamic-function studies.

Now that the clinician can use sophisticated imaging equipment and electronic computers for data treatment (*6*), it is important that he understand the fundamental limitations in gamma-ray imaging. The purpose of this paper is to discuss these basic limitations and illustrate their effect on the limiting performance of a widely used gamma-ray-imaging system.

ANALYTICAL CRITERIA

All gamma-ray imaging systems basically function by detecting gamma rays emitted by the isotope-containing organ and presenting a two-dimensional pictorial display of these detected quanta. More specifically, the imaging system is equipped with a collimating aperture that accepts a certain fraction of the quanta emitted by the organ. This aperture, or collimator, provides a gamma-ray image (in differential form for the rectilinear scanners and integral form for the stationary cameras) of the source for the radiation detector. The detector, typically of the scintillation type, is sensitive (with certain efficiency) to the quanta on an individual basis and each detected gamma ray can be registered on the image display. This display can take the form of a scintillation or dot pattern on a cathode-ray tube or television monitor, a carbon dot pattern on paper, or a photo-dot image on film. The examining physician must then interpret the scan. Although the components of the various systems may differ in exact form and function, all imaging devices can be broadly described in this manner. As such, a dot pattern is presented for interpretation.

This image recognition situation relates directly to the fundamental limitations of visual perception. This results because, in trying to minimize radiation dose for curioscopic examinations, we are attempting to maximize the diagnostic information gain while minimizing the number of required quanta. Rose (*7*) and Coltman (*8*) have shown that in visualization cases such as this the quantized nature of recorded events and the associated statistical fluctuations will set an upper limit on the amount of discernible detail in the image. These scintillation or photon-noise limitations were vividly illustrated by Rose (*9*) in a series of photographs (Fig. 1) showing the improvement of detail perception, or resolution, as the number of scintillations comprising the image increased.

For their studies on scintillation limitations in image recognition, Rose considered circular images and Coltman used a square-wave or bar pattern of scintillations displayed on a television monitor. Coltman found (*10*) that when the scene on the monitor was photographed and viewed under static conditions, the population of quanta required for pattern recognition was approximately equal to that in a 0.14-sec exposure of the live display. Since most

Received Nov. 6, 1967; revision accepted April 26, 1968.

For reprints contact: E. L. Keller, Research Laboratories, Westinghouse Electric Corp., Research and Development Center, Churchill Boro, Pittsburgh, Pa., 15235.

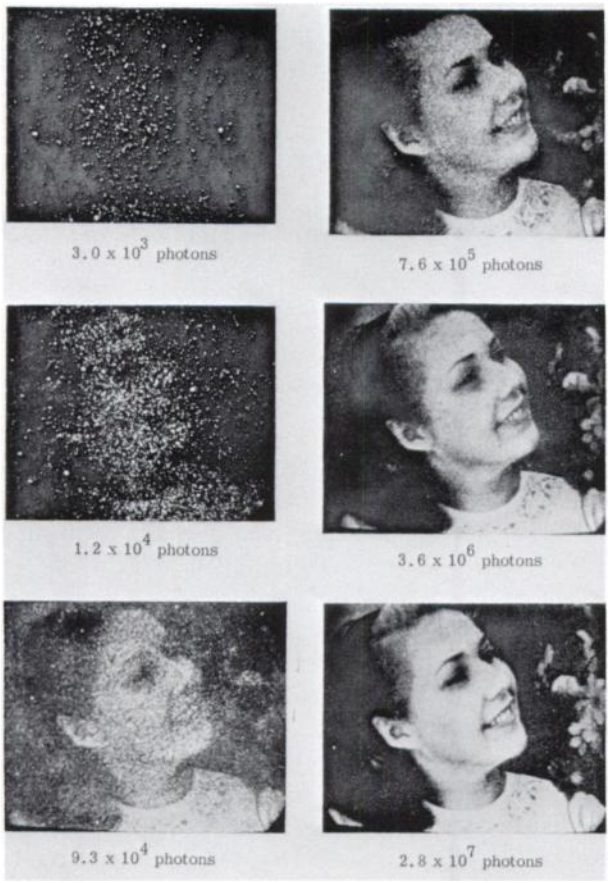

FIG. 1. Images formed by quanta (after Rose, Ref. 9). Series of photographs show improved image quality with increasing number of quanta. (Figure reproduced by permission of the Editor, *J. Opt. Soc. Am.*)

isotope scans are examined as still pictures, Coltman's findings are directly applicable.

Consider a scintillation pattern in which the population of dots per unit area varies sinusoidally with distance where α is the maximum density and β is the minimum density. The contrast for such an image is defined as the ratio of the AC component of the population density (one-half of the peak-to-peak density, $[(\alpha - \beta)/2]$) to the average density, or DC component $[(\alpha + \beta)/2]$. That is, the contrast (C) is given by

$$C = \frac{\alpha - \beta}{\alpha + \beta}. \qquad (1)$$

Coltman's experiments (*8,10*) were specifically directed towards the pattern-recognition problem in fluoroscopy. Although the results in Ref. *8* were expressed in terms of highlight population and a different definition for contrast, they can readily be recast in terms of the average population density and the contrast defined in Eq. 1. Making these changes, Coltman's results show that the total population of scintillations (P_t) required to perceive a bar pattern in a square picture was approximately

$$P_t \simeq 0.7\, N^2/C^2 \text{ (square-waves)}$$

in which N is the number of line pairs or cycles in the image and C is the contrast defined by Eq. 1. For patterns comprised of sine-wave rather than square-wave or bar patterns, one expects a factor of $(4/\pi)^2$ more scintillations to be required for equal visibility, thus yielding

$$P_t \simeq 1.1\, N^2/C^2 \text{ (sine waves)}.$$

The spatial frequency (ν) is related to N and the area of the image (A) by $\nu = NA^{-1/2}$. Consequently the limiting average scintillation density is

$$P_{av} = P_t/A \simeq 1.1\, \nu^2/C^2 \text{ (sine waves)}. \qquad (2)$$

This expression represents the fundamental scintillation limitation to the perception of images with a spatial frequency ν and a contrast C. The utility of Eq. 2 is further appreciated when it is recognized that any spatial distribution of radiation intensity (or radioisotope sources) can be considered as a superposition of sinusoidal components. Consequently, the response of an imaging system to any distribution can, in principle, be found by the superposition of the responses to the various spatial frequency components comprising the source.

It should be understood that Eq. 2 is *not* presented here as a rigid formula that has been firmly established for all pattern recognition situations of this nature. In actuality, one has a function of many variables—image size, brightness, total number of lines, experience of the observer, etc.—with a numerical coefficient reflecting these interdependent parameters. Having been useful for x-ray fluoroscopy under optimized and adjustable conditions, one might expect Eq. 2 to hold similarly for gamma-ray imaging. It is simply presented as a useful basis for understanding systems, with a coefficient that probably lies in the neighborhood of that given.

Consider a radioisotope distribution where the concentration varies sinusoidally with distance. A gamma-ray imaging system will present an image of this pattern in which the number of scintillations per unit area also varies sinusoidally with position, but typically with reduced contrast. The ratio of the image contrast (C_i) to the source contrast (C_s) is a measure of the resolution capability of the image system and is designated the contrast or modulation transfer. This modulation transfer is a function of the spatial frequency of the sine-wave pattern (e.g., cycles per unit distance). Consequently, we

obtain a modulation transfer function (MTF) for the system as

$$\text{MTF}\ (\nu) = C_i/C_s. \qquad (3)$$

Thus a given spatial frequency (i.e., resolution) in the source with a given C_s will be perceivable provided the contrast transferred to the display image is not degraded below the contrast threshold satisfying Eq. 2.

Morgan (*11*) has discussed the value of describing the informational recording capability of systems in terms of the MTF. Quite simply, since each component of an isotope imaging system affects the system's ability to record detail, it generates a MTF. The power of this Fourier method of analysis lies in the fact that the MTF of any complex system can be derived by combining those for each component, starting with the gamma-ray collimator and ending with the eye of the examining physician in the present case. It will be shown in the following that the MTF of the collimator of gamma-ray imaging systems in practice largely controls the response although that of the gamma-ray image detector in stationary cameras usually limits the ultimate resolution capability.

The MTF of the isotope-imaging system and the scintillation-limited population requirements for sine-wave pattern recognition combine naturally to determine the limiting sensitivity-resolution capability of the system. The performance of any isotope-imaging system is determined by a combination of the scintillation population recorded with the contrast loss introduced by the system. This is illustrated in Fig. 2 where the exact form of the composite curve is determined by the form of the system MTF.

In curves of this nature derived for specific imaging systems, the quantity of interest will be the product of activity in the organ and the integration time required to attain a particular resolution. Conversely, it will be possible to choose ν and ask whether the associated activity and time are reasonable in keeping with permissible radiation doses. The scintillation or dot population of the final image is related to the activity-time product by the system sensitivity as follows:

$$P = 2.2 \times 10^6\ \sigma\ y\ T\ \Omega\ I\ n\ t\ \text{dots}, \qquad (4)$$

in which

- σ is the activity in the organ, expressed in microcuries (μc),
- y is the number of useful gamma rays emitted per disintegration,
- T is the transmission probability for undeflected quanta leaving the organ *and* the body,
- Ω is the geometric acceptance of the collimator (see next section),
- I is the interaction probability of the gamma rays in the image detector,
- n is the number of dots registered in the final image per detected quantum (≤ 1) and
- t is the integration time in min.

By combining Eqs. 2, 3 and 4 we find that the limiting resolvable spatial frequency, which is the reciprocal of the maximum resolution (R), is related to the organ activity and integration time as

$$\nu = R^{-1} \simeq 1{,}400\ C_s\ \text{MTF}\ (\nu)\ (B\sigma t/A)^{1/2}, \qquad (5)$$

in which $B = y\ T\ \Omega\ I\ n$. When Eq. 5 is applied to various isotope imaging systems, the differences arise through the factors Ω, I, n, t and MTF (ν) which are system parameters. The terms C_s, σ, A, y and T are descriptive of the gamma-ray energy of the isotope and the organ of interest; these are common to all systems. We assume throughout that the area of the displayed image and the source area are equal.

SYSTEM EVALUATION CRITERIA

To illustrate the application of these criteria and their value in understanding the performance limitations of a gamma-ray imaging system, we consider the characteristics of an Anger type of scintillation camera equipped with parallel-hole multiaperture collimators. We consider this particular system for illustration because its characteristics have been the subject of recent investigation.

Geometric resolution and acceptance for parallel-hole multiaperture collimators. Following the method of Anger (*5*), we consider a rectangular array of

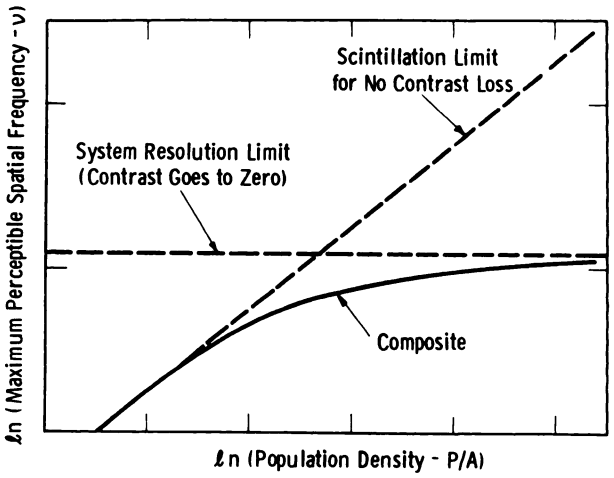

FIG. 2. Scintillation-limited performance of imaging system with a resolution limitation.

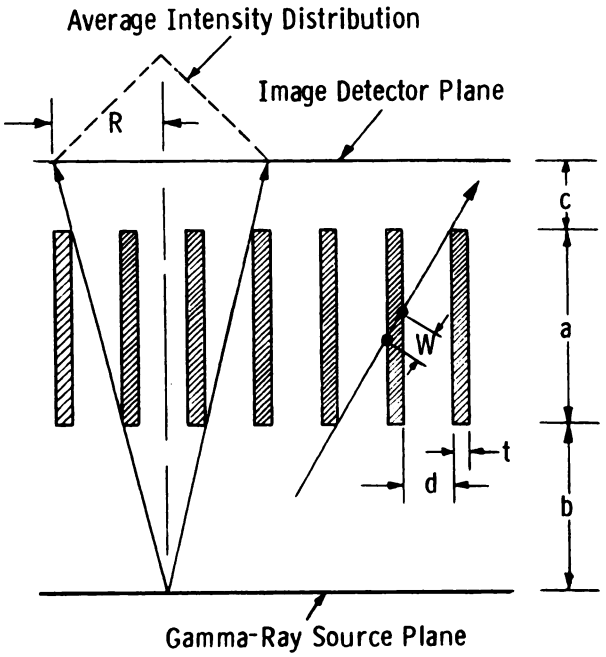

FIG. 3. Sectional view of parallel-hole multiaperture collimator shows path of minimum septal attenuation, limiting gamma-ray paths and average intensity distribution on image detector (see Ref. 5).

square holes of width d, length a and separated by septa of thickness t (Fig. 3). The source-to-collimator and collimator-to-detector distances are designated by b and c, respectively. The limiting geometric resolution (R) is defined as the full width at half maximum (FWHM) of the average intensity distribution obtained from a point source. By geometry, this is given by

$$R = d(a_e + b + c)/a_e, \tag{6}$$

in which a_e is the effective length of holes which is less than the geometric hole length because of gamma-ray penetration. This effective hole length is approximately given by (*12*)

$$a_e = a - 2\mu^{-1}, \tag{7}$$

in which μ is the linear absorption coefficient of the collimator material.

One of us has shown (*13*) that the dimensions of this type collimator can be chosen to optimize the geometric acceptance (Ω) for a given resolution (R) where Ω is defined as the ratio of the number of image-forming gamma rays transmitted by the collimator to those emitted by the source. This optimum value is

$$\Omega_{opt} = \left[\frac{6\mu KR}{(A+6)^2}\right]^2, \tag{8}$$

in which $A^2 = 6 + 6\mu\ (b + c)$ and K is a constant with the value 0.282 for square holes in a rectangular array. Equation 8 is derived using the approximation that $a \gg 2d + t$ (applicable for most practical collimators) and choosing t so that the gamma-ray transmission for the minimum penetration path W in Fig. 3 is some small percentage such as 5%, i.e., $\exp(-\mu W) = 0.05$ or $\mu W = 3$. The value Ω_{opt} is simply the maximum of

$$\Omega = [Kd^2/a_e(d + t)]^2 \tag{9}$$

as a function of the hole length (a) and occurs at an optimum hole length (a_{opt}) given by

$$a_{opt} = (A + 3)\mu^{-1}. \tag{10}$$

This value is independent of the resolution R. In association with a_{opt}, the other optimum dimensions of the collimator are dependent on R and are given by

$$d_{opt} = R(a_{opt} - 2\mu^{-1})/(a_{opt} - 2\mu^{-1} + b + c) \tag{11}$$

and

$$t_{opt} = 6\ d_{opt}/(\mu a_{opt} - 3). \tag{12}$$

Modulation transfer function. The two-system components of a stationary camera which most affect resolution and the MTF are the collimator and the gamma-ray image detector. The image detector MTF is actually comprised of several components including the gamma-ray detector, the spatial information transfer system and the image display. In several recent measurements (*14,15*) these factors together with the eye of the examiner were combined to yield an over-all image detector MTF. As such, we define the total system MTF as

$$\text{MTF}\ (\nu)]_s = \text{MTF}\ (\nu)]_{coll} \times \text{MTF}\ (\nu)]_{id}, \tag{13}$$

in which the subscripts s, coll and id refer to the total system, collimator and image detector, respectively.

Most of the early measurements concerning the intrinsic resolution of the image detector for the Anger type of scintillation camera were related to the minimum separation of either two point (*16*) or line (*17*) sources for which a barely-resolved image could be discerned. This separation, designated the intrinsic resolution (R_i), is a function of the gamma-ray energy and has values of 13 mm at 70 kev, 10 mm at 140 kev, 7.1 mm at 279 kev and 6.4 mm at 364 kev for a system equipped with bialkali photocathodes (*17*). Several more recent studies (*14,15*) have provided $\text{MTF})_{id}$ directly by measuring the line-spread function and taking its Fourier transform. These data indicate that the line-spread

function is nearly Gaussian in shape with a FWHM given approximately by R_i. Since the Fourier transform of a Gaussian line-spread function yields a Gaussian MTF, we assume hereafter that the $MTF)_{id}$ of the Anger system can be approximated by

$$MTF)_{id} = \exp(-2\pi^2\sigma^2\nu^2), \quad (14)$$

in which $R_i = 2.354\ \sigma$.

The MTF of a parallel-hole, multiaperture collimator is obtained from the fact that the average point-source response function, p(x,y), is conical in shape (*5*), i.e.,

$$p(x,y) = \frac{3}{\pi R^3}\left[R - (x^2 + y^2)^{1/2}\right]. \quad (15)$$

The line-spread function, l(x), is defined by

$$l(x) = \int_{-\infty}^{\infty} p(x,y)\, dy \quad (16)$$

and for the particular function defined by Eq. 15,

$$l(x) = \frac{3}{\pi R}\left\{\left[1 - (x/R)^2\right]^{1/2} - \frac{1}{2}\left(\frac{x}{R}\right)^2 \ln\left[\frac{1 + [1 - (x/R)^2]^{1/2}}{1 - [1 - (x/R)^2]^{1/2}}\right]\right\} \quad (17)$$

The MTF or Fourier transform is obtained by the integration.

$$MTF(\nu) = \int_{-\infty}^{\infty} l(x)\, \exp(2\pi i \nu x)\, dx. \quad (18)$$

Because of the nature of Eq. 17, its MTF is obtained by a series approximation (*18*). The spatial frequency (ν) is that in the gamma-ray image plane and also the source plane since this type collimator images one-to-one.

Scattered radiation. A major problem in the attainment of an optimal-information isotope image is that of scattered radiation. A gamma ray produced in the isotope-containing organ can leave the organ and surrounding tissue without interaction, be accepted by the collimator, detected by the system and finally registered in the output image at a position in direct correspondence with its point of origin. This is the ideal situation. However, quanta emitted in directions not acceptable by the collimator can be scattered into an acceptable direction, detected and registered. This scattering can occur in the organ, surrounding tissue (or bones) or any material associated with the detector, e.g., the collimator or the detecting phosphor itself. The positions in the final image for these quanta will correspond with the scattering positions and not the quantum origins. The net result is that contrast is degraded and information lost. The attainment of a given resolution will consequently require many more quanta because of the C^{-2} dependence in Eq. 2.

Scattered radiation can be rejected using pulse-height analysis, which refers to the energy analysis of the detected quanta in pulse radiation detectors. This accrues because the gamma ray loses energy in the scattering process. Thus by analyzing the energy of the detected quanta and registering only those with full energy, this source of contrast degradation can be reduced. This is accomplished in various systems with varying degrees of success, in part due to the kinetics of the Compton scattering process (*19*) and the finite width of the photopeak window of the gamma-ray spectrometer (*5*). These limitations are generally more detrimental at the lower gamma-ray energies ($\lesssim 100$ kev) (*20*).

As Beck and Harper have indicated (*21*), it is theoretically immaterial whether the scattered radiation is considered to reduce the system MTF or the initial source contrast. In either case, the net effect on the image contrast in the final display is the same.

RESULTS

We can now use the considerations discussed above to predict the scintillation-limited performance of any gamma-ray imaging system. Specifically we shall demonstrate this application for the Anger type of scintillation camera. Before doing this, however, it will be instructive to discuss several qualitative aspects of this procedure.

The maximum resolvable spatial frequency is given by Eq. 5. By rearranging the terms of this equation, we obtain

$$\sigma t \simeq \frac{A}{2.0 \times 10^6\, B}\, \frac{\nu^2}{C_s^2[MTF(\nu)]^2}. \quad (19)$$

Hence by specifying a value for ν, knowledge of the system and specific isotope-organ parameters under consideration permits the calculation of the required σt for that frequency. For example, we can consider a camera equipped with a coarse-resolution collimator such that the resolution capability of the image detector is not a limiting factor, i.e., $MTF)_{id} \simeq 1$ for ν less than $\nu_{lim} = R^{-1}$, where R is the limiting geometric resolution of the collimator (Eq. 6). We now choose several values of ν between $\sim 0.05\ \nu_{lim}$ and ν_{lim} and calculate σt for each using Eq. 19 which defines a curve on a ν versus σt plot as labeled "a" in Fig. 4. This curve is shaped similarly to that labeled "composite" in Fig. 2. Next we repeat this for a collimator with better resolution (i.e., smaller R). Since R is smaller, the resultant curve b is shifted to greater σt products because of the dependence of Ω on R^2 (Eq. 8), but extends to higher ν because of the improved $MTF)_{coll}$. By continuing

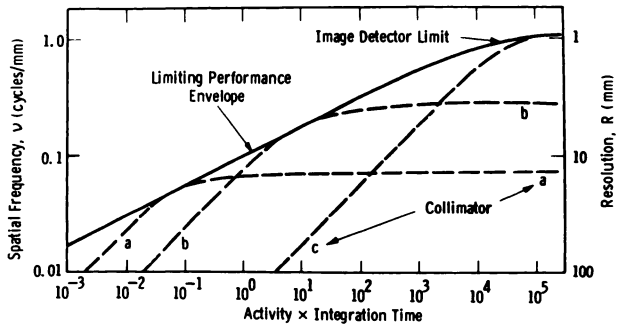

FIG. 4. Limiting performance of gamma-ray imaging system as affected by image detector and acceptance and resolution of different collimators.

this with smaller and smaller R values, we reach frequencies where $MTF)_{id}$ becomes a limitation and must be coupled with $MTF)_{coll}$ for use in Eq. 19. This would occur for a collimator associated with curve c in Fig. 4.

A series of these curves for different collimators can be connected by an envelope which defines the combined limiting performance of the system independent of the particular optimum collimator considered. In essence, the consideration of this envelope eliminates the need to discuss a wide variety of collimators when comparing the limiting performance of various systems. Since optimized collimators are common to most stationary systems, the envelope removes this factor from over-all comparisons.

The limiting performance envelope varies as the fourth power of ν in the region where $MTF)_{id} \simeq 1$; one quadratic factor comes from the population equation and a second is due to the dependence of Ω_{opt} on R^2 (Eq. 8). The fall-off of the envelope near the image detector limit is proportional to $[MTF)_{id}]^2$.

It should be noted that the curve for a given collimator touches the envelope at only one point and this is the optimum frequency or resolution for that collimator. This optimum frequency depends on the specific form of $MTF)_{coll}$ and the specific dependence of Ω on R. We find graphically that $\nu_{opt} \simeq 0.40\ R^{-1}$ for parallel-hole multiaperture collimators. This means that a collimator with a limiting resolution of R_{coll} is optimally used in attaining a source resolution of 2.5 R_{coll}. Beck and Harper (*21*) have obtained a similar result for rectilinear scanners.

Specific system, isotope and organ characteristics. The following characteristics were considered in applying the present analysis to the Anger type of scintillation camera for imaging several isotopes in the brain.

Anger camera

a. Calculated values of the photopeak detection efficiency (*22*) for a ½-in.-thick NaI(Tl) crystal were used for I in Eq. 5 (or 19).
b. Recent intrinsic resolution measurements (*17*) with a system equipped with bialkali photomultiplier tubes were used for R_i associated with $MTF)_{id}$ (Eq. 14).
c. Lead was considered for all collimator materials.
d. It was assumed that each photopeak detection event was displayed in the final image, i.e., $n = 1$ in Eq. 5.
e. Pulse-height analysis was assumed perfect so that scattered radiation had no effect on the final image.
f. The collimator-to-detector distance c associated with parallel-hole multiaperture collimation was taken to be $1\frac{1}{32}$ in.; a $\frac{3}{32}$-in. air gap plus ¼ in. to the center of the ½-in.-thick crystal.

Isotopes

a. The isotopes considered for these illustrative comparisons were ^{131}I, ^{113m}In and ^{99m}Tc.
b. Values for y in Eq. 5, the number of useful gamma rays per disintegration, were taken from Smith (*23*) and Strominger, Hollander and Seaborg (*24*).
c. Maximum administerable activities were taken from the tabulation of Silver (*25*).
d. An uptake of 5% for the brain was assumed.

Organs

a. The brain was considered for illustration and typical organ dimensions [courtesy of Professor Y. Wang (*26*)] used were 220 cm^2 for the area and 8.5 cm for the midplane depth.
b. Resolutions were calculated at the organ midplane and average attenuations (T in Eq. 5) were calculated at that position.

Limiting performance curves. Using the parameters discussed above, we illustrate the modulation-transfer and scintillation limitations in gamma-ray imaging for the Anger type of scintillation camera. In presenting a limiting performance curve for a system equipped with a particular collimator (Eq. 19) or the limiting performance envelope defined by a series of these individual curves, it is more convenient to plot them for a source contrast (C_s) of unity. Thus any source contrast can be considered simply by displacing the curve to the right (to greater σt products) by a factor of C_s^{-2}, or, analogously, by shifting the values of the abscissa to the left by the same factor. For example, a source contrast of

31.6% would require an abscissa shift by a factor of $(0.316)^{-2} = (0.10)^{-1} = 10$.

First we consider the Anger system for imaging the brain using ^{99m}Tc. Anger has described (*27*) a special collimator designed for this purpose which provides a limiting geometric resolution (Eq. 6) of R = 13.1 mm at a midplane depth of 8.5 cm. An optimized lead collimator (*13*) with this limiting resolution has $\Omega_{opt} = 8.6 \times 10^{-4}$. By using the associated collimator MTF and that for the intrinsic resolution of R_i = 10 mm (140 kev) in Eq. 19, we obtain the curve labeled R_{coll} = 13.1 mm in Fig. 5. As expected, this curve approaches the limiting collimator resolution of ~13 mm at very high σt products.

We can now ask, "What is the best source resolution we could attain with this particular collimator?" The answer, of course, depends on four factors: the maximum administerable activity, the uptake, the source contrast and the integration time. If we consider σ = 15 mc, an uptake of 5%, C_s = 31.6% and t = 10 min, this gives us a point at 15,000 μc × 0.05 × $(0.316)^2$ × 10 min = 750 μc-min, indicated by the open circle. This occurs at ν = 0.062 cycles/mm or R = $1/\nu$ = 16.1 mm. This is the best source resolution attainable for this collimator and the stated conditions.

The statement often appears that the collimator of the Anger system, not the image detector, was limiting the resolution in a particular application. This would be true for the above example, but *unnecessarily* so, particularly when high photon yields from isotopes such as ^{99m}Tc are available. The limiting performance envelope in Fig. 5 shows that a source resolution of 12.2 mm is attainable with the proper collimator. As discussed previously, the best R_{coll} to attain this would be 12.2/2.5 = 4.9mm. Although such a collimator would have $\Omega_{opt} = 1.2 \times 10^{-4}$, a factor of seven smaller than that for the R_{coll} = 13.1 mm collimator, its higher MTF permits the over-all system performance to approach the image-detector resolution limitation. Actually, the R_{coll} = 13.1 mm collimator is only optimal for imaging in the vicinity of 0.03 cycles/mm where R = 2.5 R_{coll} = 33 mm as is indicated by its curve touching the envelope at that point.

This analytical formulation is also useful in comparing the use of different isotopes for imaging the same organ. For example, we plot in Fig. 6 the limiting performance envelopes for both ^{131}I and ^{99m}Tc. For ^{131}I we consider σ = 300 μc and, as before, an uptake of 5%, C_s = 31.6% and t = 10 min. This yields σt = 15 μc-min and provides a maximum resolution of only 19.4 mm, considerably worse than that of 12.2 mm with ^{99m}Tc. Consequently, we see that ^{131}I cannot compete with ^{99m}Tc, even though the intrinsic resolution of the image detector is better for this higher energy isotope (E_γ = 364 kev). The low photon yield from ^{131}I prevents the use of this better resolution, which is available only for $\sigma t \lesssim 80$ μc-min.

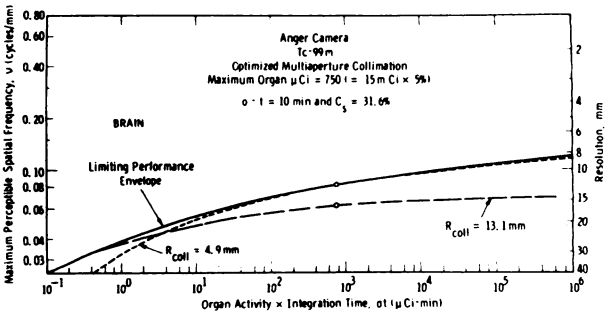

FIG. 5. Limiting performance curves for brain using ^{99m}Tc. Curves are drawn for source contrast (C_s) of unity. Open circles on curves refer to combination of t = 10 min and C_s = 31.6% for maximum organ activity.

The newly-available ^{113m}In isotope (*28*) is a high-energy-gamma isotope (392 kev) which does not have this photon-yield limitation. Figure 6 also shows the limiting performance envelope for ^{113m}In; it is near that of ^{131}I because of the close photon energies. However, ^{113m}In is similar to ^{99m}Tc in its characteristics so that administered activities can be similar. Thus the 750 μc-min point for ^{113m}In actually provides slightly better resolution than ^{99m}Tc. This is simply a manifestation of the fact that the $MTF)_{id}$ of the Anger system favors the higher-energy-gamma isotopes. Even though the collimator and detection efficiency favor low-energy-gamma isotopes, the $MTF)_{id}$ is the dominant factor for the Anger system in the high-photon-yield region.

DISCUSSION OF RESULTS

By applying this analysis to the Anger type of scintillation camera, we have illustrated its utility for

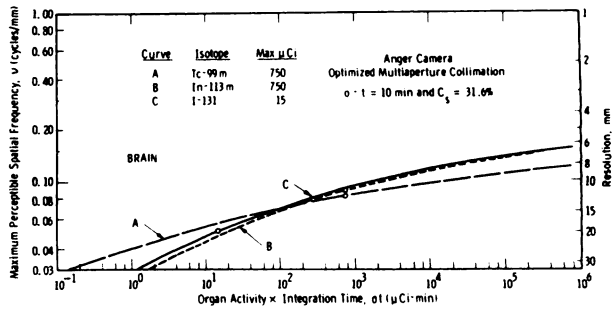

FIG. 6. Limiting performance envelopes for brain using different isotopes. Curves are drawn for source contrast (C_s) of unity. Open circles on curves refer to combination of t = 10 min and C_s = 31.6% for maximum organ activities.

providing insight to the system's fundamental features and guidance for its effective use in clinical practice. Several conclusions can be drawn from this particular illustration:

1. The relatively coarse resolution collimators provided with the Anger system for imaging low-photon-yield isotopes such as ^{131}I and ^{203}Hg are probably adequate for most applications.
2. For use with high-photon-yield isotopes, however, high-resolution collimators should be provided which give resolutions limited by the intrinsic resolution of the image detector.
3. Further gains in resolution might then be possible by improving the intrinsic resolution of the image detector if physically possible.

It would be ideal, of course, to use experimentally determined MTF's when analyzing this or any system. It is particularly important to know how scattering affects the MTFs or, analogously, how it affects the initial source contrast as transferred by the collimator to the image detector. This is important because the capability of various systems for rejecting scattered radiation can differ markedly (*21,29*). It is encouraging that data of this type are appearing for some of the newer systems.

CONCLUSIONS

We have discussed the modulation-transfer and scintillation limitations in gamma-ray imaging and have illustrated their effect on the limiting performance of a widely used scintillation camera. This particular formulation combines the interdependent factors of resolution and sensitivity through the system modulation transfer function and the fundamentals of image perception. It is very useful for gaining an understanding of those factors which limit the performance of a given system and for comparing systems.

The analysis is perfectly general and can be applied to any gamma-ray imaging device. Care must be exercised, however, when intercomparing systems. For example, the collimation characteristics of focused collimators used with rectilinear scanners differ from those for parallel-hole multiaperture collimators used with cameras. This is so because, aside from sectional scanning, most systems present a two-dimensional image of a three-dimensional object. Other differences can arise from different display systems and are related to subjective interpretation by the examiners.

In discussing this over-all problem, we have approached it from the limiting or optimum performance standpoint by considering a series of optimized collimators. We realize, however, that this ideal flexibility is not normally available to the clinician —his scanning instrument may be equipped with only two or three collimators. Notwithstanding, the present analysis will yield a plot of ν (or R) as a function of σt for each system configuration (such as curves a or b in Fig. 4) which can help him to understand his system and the most efficient tradeoffs among resolution, activity and integration time available to him.

The concepts of modulation transfer function and scintillation limitations to image perception are relatively new to the isotope imaging area of nuclear medicine although they have been applied to x-ray radiography for many years. The recent analyses of Beck and Harper incorporate these concepts and have the same qualitative features as the present formulation. The plots of R as a function of σt obtained from the present considerations (Eq. 19) do represent a new and powerful aid for understanding gamma-ray imaging systems. Additional investigation, both theoretical and experimental, is needed. Certainly the recently-initiated studies by Schulz and co-workers (*30,31*) on the computer simulation of data from scanning systems will shed light on this important problem.

REFERENCES

1. COPELAND, D. E. AND BENJAMIN, E. W.: Pinhole camera for gamma-ray sources. *Nucleonics* **5**:No. 8, 44, 1949.

2. ANGER, H. O.: Use of a gamma-ray pinhole camera for in vivo studies. *Nature* **170**:200, 1952.

3. CASSEN, B., CURTIS, L., REED, C. AND LIBBY, R.: Instrumentation for I-131 use in medical studies. *Nucleonics* **9**:No. 8, 46, 1951.

4. Curioscopy is the detection and mapping of objects by the nuclear radiations coming from them. See R. R. Newell, "Curioscopy" in *Medical Physics* vol. 3, ed. by Glasser, Year Book Publishers, Chicago, 1960, p. 211.

5. ANGER, H. O.: Radioisotope cameras, in *Instrumentation in Nuclear Medicine* vol. 1 ed. by G. J. Hine, Academic Press, New York, 1967, p. 485.

6. SMITH, E. M. AND BRILL, A. B.: Progress with computers in nuclear medicine. *Nucleonics* **25**:No. 5, 64, 1967.

7. ROSE, A.: Sensitivity performance of the human eye on an absolute scale. *J. Opt. Soc. Am.* **38**:196, 1948.

8. COLTMAN, J. W.: Scintillation limitations to resolving power in imaging devices. *J. Opt. Soc. Am.* **44**:234, 1954.

9. ROSE, A.: Quantum and noise limitations of the visual process. *J. Opt. Soc. Am.* **43**:715, 1953.

10. COLTMAN, J. W.: unpublished data.

11. MORGAN, R. H.: Frequency response function. *Am. J. Roentgenol., Rad. Therapy and Nuclear Med.* **88**:175, 1962.

12. MATHER, R. L.: Gamma-ray collimator penetration and scattering effects. *J. Appl. Phys.* **28**:1,200, 1957.

13. KELLER, E. L.: Optimum dimensions of parallel hole, multiaperture collimators for gamma-ray cameras. To be published.

14. CRADDUCK, T. D., FEDORUK, S. O. AND REID, W. B.: New method of assessing the performance of scintillation cameras and scanners. *Phys. Med. Biol.* **11**:423, 1966.

15. COHEN, T.: Personal communication.

16. MYERS, M. J., KENNY, P. J., LAUGHLIN, J. S. AND LUNDY, P.: Quantitative analysis of data from scintillation cameras. *Nucleonics* **24**:No. 2, 58, 1966.

17. ANGER, H. O.: Sensitivity, resolution and linearity of the scintillation camera, *IEEE Trans.* **NS-13**:380, 1966.

18. BECK, R. N.: Scanning system as a whole: general considerations, in *Fundamental Problems in Radioisotope Scanning* ed. by A. Gottschalk and R. N. Beck. To be published.

19. See, for example, EVANS, R. D.: *The Atomic Nucleus,* McGraw-Hill Book Co., New York, 1955, Chapter 23.

20. ROSS, D. A., HARRIS, C. C., SATTERFIELD, M. M., BELL, P. R. AND JORDAN, J. C.: "Low-energy gamma emitters in scanning and other clinical applications, in *Radioaktive Isotope in Klinik und Forschung* vol. 6, ed. by K. Fellinger and R. Höfer, Urban and Schwarzenberg, Berlin, 1965, p. 108.

21. BECK, R. N. AND HARPER, P. V.: Criteria for evaluating radioisotope imaging systems. To be published.

22. ANGER, H. O. AND EVANS, D. H.: Gamma-ray detection efficiency and image resolution in sodium iodide. *Rev. Sci. Instr.* **35**:693, 1964.

23. SMITH, E. M.: Calculating absorbed doses from radiopharmaceuticals. *Nucleonics* **24**:No. 1, 33, 1966.

24. STROMINGER, D., HOLLANDER, J. M. AND SEABORG, G. T.: Table of isotopes. *Rev. Mod. Phys.* **30**:585, 1958.

25. SILVER, S.: Uses of radioisotopes in medicine. *Nucleonics* **23**:No. 8, 106, 1965.

26. WANG, Y.: Personal communication.

27. ANGER, H. O.: Scintillation camera with multiaperture collimators. *J. Nucl. Med.* **5**:515, 1964.

28. STERN, H., GOODWIN, D., WAGNER, H. N., JR. AND KRAMER, H.: In^{113m}—A short-lived isotope for lung scanning. *Nucleonics* **24**:No. 10, 57, 1966.

29. GOTTSCHALK, A.: Modulation transfer function for cameras, in *Fundamental Problems in Radioisotope Scanning* ed. by A. Gottschalk and R. N. Beck. To be published.

30. SCHULZ, A. G., KOHLENSTEIN, L., KNOWLES, L. G., YATES, W. A. AND MUCCI, R. F.: Quantitative assessment of scanning system parameters. *J. Nucl. Med.* **8**:284, 1967.

31. KOHLENSTEIN, L. C., SCHULZ, A. G., MUCCI, R. F. AND KNOWLES, L. G.: Simulation of data from scan detector systems. *J. Nucl. Med.* **8**:312, 1967.